NK3 homeobox 1 (NKX3.1) up-regulates forkhead box O1 expression in hepatocellular carcinoma and thereby suppresses tumor proliferation and invasion

Received for publication, April 28, 2017, and in revised form, September 22, 2017 Published, Papers in Press, September 27, 2017, DOI 10.1074/jbc.M117.793760

Jingyi Jiang[‡§1], Zheng Liu[‡§1], Chao Ge[§], Cong Chen[§], Fangyu Zhao[§], Hong Li[§], Taoyang Chen[¶], Ming Yao[§], and Jinjun Li[§2]

From the [‡]Shanghai Medical College, Fudan University, Shanghai 200032, the [§]State Key Laboratory of Oncogenes and Related Genes, Shanghai Cancer Institute, Renji Hospital, Shanghai Jiaotong University School of Medicine, Shanghai 200032, and the [¶]Qi Dong Liver Cancer Institute, Qi Dong 226200, China

Edited by Eric R. Fearon

Hepatocellular carcinoma (HCC) is the leading cause of cancer-related mortality in China, and the molecular mechanism of uncontrolled HCC progression remains to be explored. NK3 homeobox 1 (*NKX3.1*), an androgen-regulated prostate-specific transcription factor, suppresses tumors in prostate cancer, but its role in HCC is unknown, especially in hepatocellular carcinoma. In the present study, the differential expression analyses in HCC tissues and matched adjacent noncancerous liver tissues revealed that NKX3.1 is frequently down-regulated in human primary HCC tissues compared with matched adjacent noncancerous liver tissues. We also noted that NKX3.1 significantly inhibits proliferation and mobility of HCC cells both *in vitro* and *in vivo*. Furthermore, NKX3.1 overexpression resulted in cell cycle arrest at the G_1/S phase via direct binding to the promoter of forkhead box O1 (*FOXO1*) and up-regulation of expression. Of note, FOXO1 silencing in NKX3.1-overexpressing cells reversed the inhibitory effects of NKX3.1 on HCC cell proliferation and invasion. Consistently, both FOXO1 and NKX3.1 were down-regulated in human HCC tissues, and their expression was significantly and positively correlated with each other. These results suggest that *NKX3.1* functions as a tumor suppressor in HCC cells through directly up-regulating FOXO1 expression.

Hepatocellular carcinoma (HCC),[3] the most common cancer in Eastern as well as in the Western countries, is one of the leading causes of death from cancer worldwide (1). HCC accounts for about 90% of primary liver malignant tumors and is known with poor prognosis (the ratio of mortality to incidence is 0.95) (2, 3). These observations highlight the urgent need for improved understanding and effective treatment for this deadly disease. Although much is known about genes involved in HCC progress, the molecular mechanism of uncontrolled HCC development remains to be explored. Transcription factors, as the components of regulating genes expression, become particularly important in cancer research.

Chromosome 8p21 is a region reported to associate with tissue de-differentiation and chr8p loss is the most frequent genomic alteration in the progression of cancers, such as prostate adenocarcinoma and lung cancer (4–7). NK3 homeobox 1 (*NKX3.1*), mapping to the human chromosome 8p21.2 region, is an androgen-regulated prostate-specific transcription factor (7, 8). *NKX3.1* is required for normal prostate development and expressed at all stages of prostate differentiation whereas its loss-of-function has been implicated in prostate cancer initiation (9–12). Furthermore, the tumor suppressor properties of *NKX3.1* are demonstrated by its ability of suppressing cell proliferation and migration as well as reducing tumorigenicity (13, 14). Additionally, NKX3.1 could activate the cellular response to oxidation and accelerate DNA repair after androgen-induced transcription to exert tumor suppressive effects in prostate cancer (15, 16).

In contrast to the researches focused on prostate cancer, the function and role of NKX3.1 in other cancers were rarely reported. In breast cancer, Bhatt and colleagues (17) showed that NKX3.1 repressed Oct-4 expression in MCF-7 cells and TOT treatment appeared to elevate NKX3.1 degradation through a p38 MARK-dependent phosphorylation of E3 ligase and SKP2. Miyaguchi *et al.* (18) found that loss of *NKX3.1* is a significant risk factor to decrease the disease-free survival and the overall survival rates of oral squamous cell carcinoma patients with cervical lymph node metastasis. This suggests NKX3.1 may be a potential biomarker for occult lymph node metastasis of oral squamous cell carcinoma (18). Moreover, the function and molecular mechanism of NKX3.1 have never been reported in HCC. Whether NKX3.1 plays a suppressive role in HCC is worthy to explore in this study.

Our work identified *FOXO1* as the direct target of NKX3.1. The forkhead box class O transcription factors play

This work was supported in part by National Natural Science Foundation of China Grant 81472726, National Key Sci-Tech Special Project of China Grant 2013ZX10002-011, and SKLORG Research Foundation Grant 91-15-03. The authors declare that they have no conflicts of interest with the contents of this article.

This article contains supplemental Figs. S1–S5 and Tables S1–S6.

[1] Both authors contributed equally to this work.

[2] To whom correspondence should be addressed: 25/Ln 2200 Xietu Rd., Shanghai 200032, China. Tel.: 86-21-64432140; E-mail: jjli@shsci.org.

[3] The abbreviations used are: HCC, hepatocellular carcinoma; NKX3.1, NK3 homeobox 1; FOXO1, Forkhead box O1; CDK2, cyclin-dependent kinase 2; RB, retinoblastoma 1; NC, negative control; qRT, quantitative RT; MTT, 3-(4,5-dimethylthiazol-2-yl)-2,5-diphenyltetrazolium bromide; NOD, non-obese diabetic; SCID, severe combined immunodeficiency.

© 2017 by The American Society for Biochemistry and Molecular Biology, Inc. Published in the U.S.A.

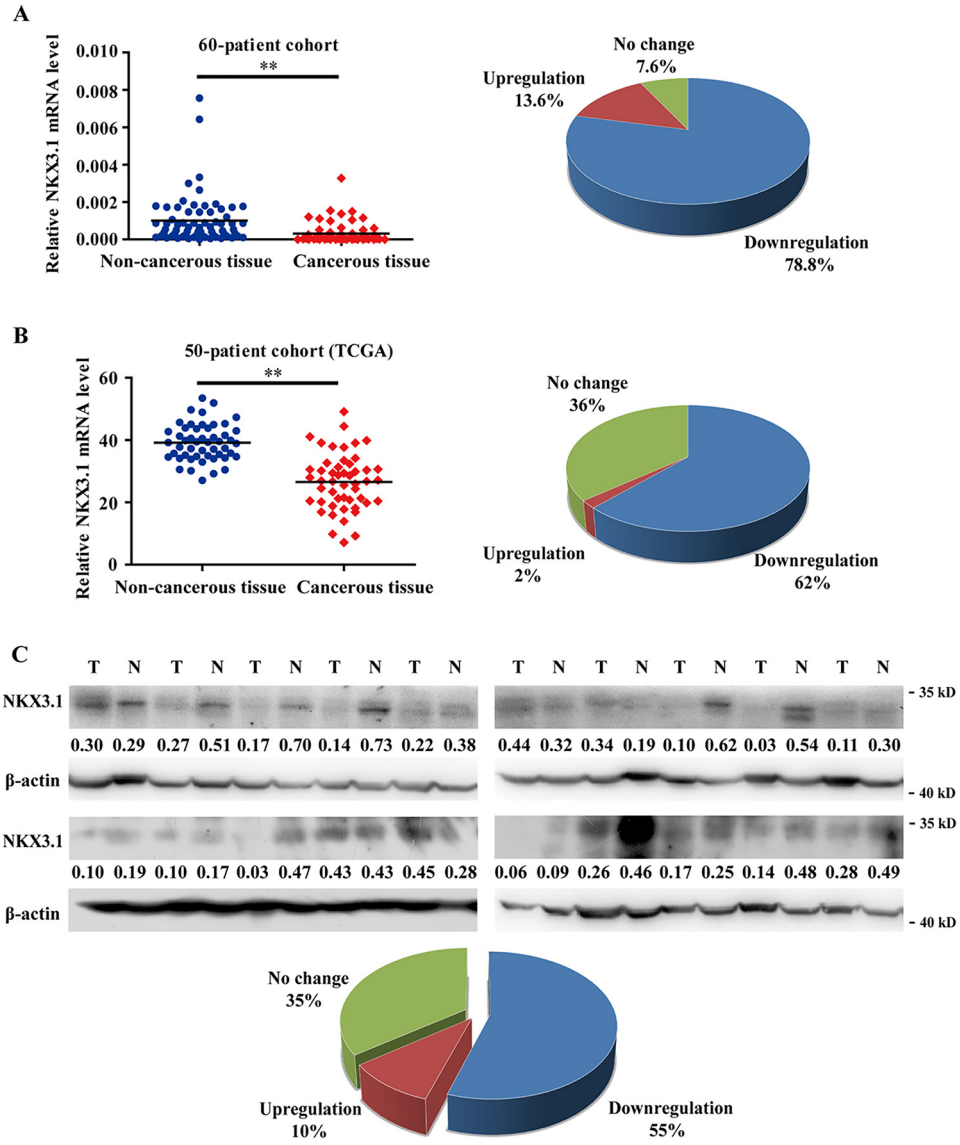

Figure 1. NKX3.1 was down-regulated in human primary HCC tissues. *A,* qRT-PCR was performed to detect *NKX3.1* mRNA expression in human primary HCC tissues and matched adjacent noncancerous liver tissues ($n = 60$, *left panel*). The *pie chart* represents the change of *NKX3.1* mRNA levels in HCC samples that exhibited up-regulation, no change, and down-regulation (*right panel*). *B,* mRNA levels of *NKX3.1* in HCC tissues and matched adjacent noncancerous liver tissues from TCGA cohort ($n = 50$, *left panel*). The *pie chart* represents the change in *NKX3.1* levels in HCC tissues that exhibited up-regulation, no change, and down-regulation (*right panel*). *C,* NKX3.1 protein levels in human primary HCC tissues (*T*) and the corresponding adjacent non-cancerous liver tissues (*N*). β-Actin was used as a loading control ($n = 20$). The protein expression levels were quantified by densitometry and calculated as the ratio of the interest protein to its loading control with ImageJ software. The *pie chart* represents the change in NKX3.1 protein levels in HCC tissues that exhibited up-regulation, no change, and down-regulation. **, $p < 0.01$.

an important role in apoptosis, cell cycle control, autophagy, and antioxidant response (19). Forkhead box O1 (*FOXO1*) is a member of forkhead transcription factor family, acts as a tumor suppressor in various carcinomas including in HCC, and its expression is negatively correlated with tumor progression (20–23).

In this study, we performed functional studies to determine the role of NKX3.1 in human primary HCC. We also integrated flow cytometry analysis, luciferase reporter assay, and ChIP assay results to reveal its potential molecular mechanism in HCC. We found that NKX3.1 was down-regulated in HCC tissues compared with matched adjacent noncancerous liver tissues. *NKX3.1* functions as a tumor suppressor in terms of cell proliferation and motility in HCC. It is also the first time to characterize FOXO1 as a direct and functional binding target of *NKX3.1* in HCC cells.

Results

NKX3.1 expression is down-regulated in HCC tissues

As the suppressor role of NKX3.1 in prostate cancer, the association between *NKX3.1* and HCC is still unknown. To address this, we tested *NKX3.1* mRNA expression in 60 pairs of human primary HCC tissues and matched adjacent noncancerous liver tissues by quantitative (q) RT-PCR. The results showed that *NKX3.1* mRNA expression was frequently down-regulated in HCC tissues compared with matched adjacent noncancerous liver tissues ($p < 0.001$; Fig. 1*A*). This is in agree-

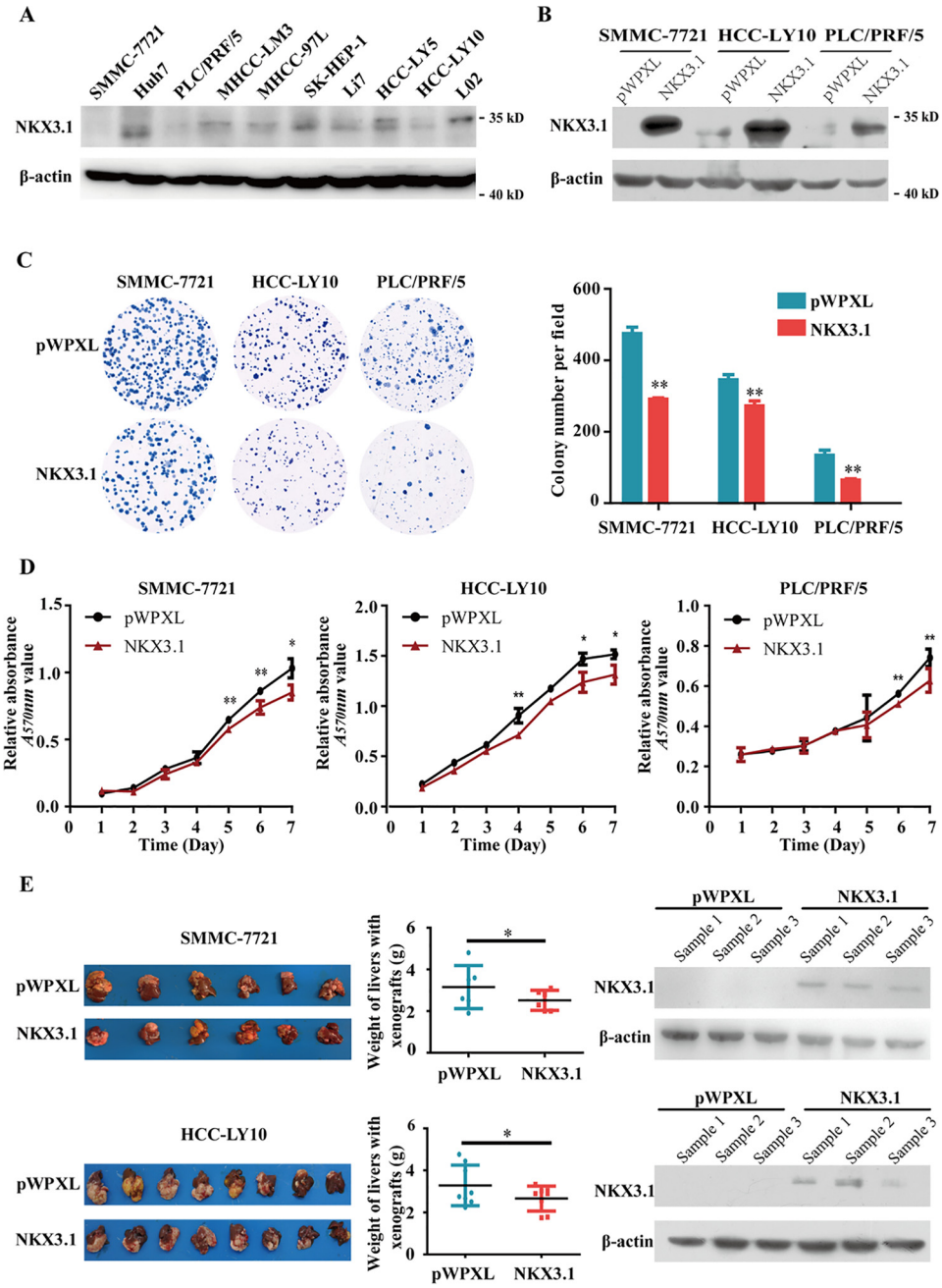

Figure 2. Overexpression of NKX3.1 inhibits HCC cell proliferation and tumorigenicity *in vitro* and *in vivo*. *A,* Western blot analysis of NKX3.1 expression in HCC cell lines and immortalized normal hepatocyte L02. *B,* Western blot analysis of NKX3.1 protein in SMMC-7721, HCC-LY10, and PLC/PRF/5 cells stably transfected with *NKX3.1* or control (*pWPXL*) vectors. *C,* overexpression of NKX3.1 inhibited the colony formation ability of HCC cells. The bar graph showed quantitative analysis data with three replicates. *D, NKX3.1* inhibited the proliferation of HCC cells by MTT assay. *E,* liver tissues collected from NOD/SCID mice with tumor xenografts inoculated with SMMC-7721 (*top panel*) and HCC-LY10 (*bottom panel*) cell lines stably overexpressing *NKX3.1*, the livers with xenografts were weighted (*left* and *middle panel*). The NKX3.1 protein level was detected by Western blot in tissue samples of xenografts (*right panel*). β-Actin was used as a loading control. *, $p < 0.05$; **, $p < 0.01$.

ment with the analysis of The Cancer Genome Atlas ($p < 0.001$; Fig. 1*B*). Western blotting analyses were also performed and showed that the NKX3.1 protein level was markedly higher in noncancerous liver tissues (Fig. 1*C*). In addition, NKX3.1 expression levels are inversely correlated with serum AFP levels ($p < 0.001$), histological grade ($p = 0.030$), and pathological stage ($p = 0.159$, no significance) in TCGA cohort (supplemental Table S5). Therefore, these findings indicate that lower expression levels of NKX3.1 are associated with the malignant progression of HCC and it is seriously possible that NKX3.1 plays a key role in the development of HCC.

Overexpression of NKX3.1 inhibits HCC cell proliferation and tumorigenesis in vitro and in vivo

We thus measured endogenous mRNA and protein expressions of *NKX3.1* in HCC cell lines and normal hepatocyte L02 (Fig. 2*A* and supplemental Fig. S1). *NKX3.1* mRNA and protein expressions were barely detected in most HCC cell lines,

whereas the expression level was higher in immortalized normal hepatocyte L02. To determine the biological function of NKX3.1 in HCC, we selected SMMC-7721, HCC-LY10, and PLC/PRF/5 to infect lentiviral vector containing complete ORF of *NKX3.1* and successfully established stable HCC cell lines with NKX3.1 overexpression (Fig. 2*B*), which were then used in functional experiments. As a control, cells were infected with empty vector pWPXL in the meantime. The plate colony formation assay and MTT assay for cell viability indicated that overexpression of NKX3.1 inhibits HCC cell proliferation *in vitro* (Fig. 2, *C* and *D*).

We then tested whether NKX3.1 displayed inhibitory ability of tumorigenesis *in vivo*. For this, stable SMMC-7721 and HCC-LY10 cells with NKX3.1 overexpression were, respectively, transplanted into the livers of non-obese diabetic/severe combined immunodeficiency (NOD/SCID) mice orthotopically. Cells transfected with empty vector pWPXL served as a control. The livers were separated from the mice after 4 weeks. Our results indicated that the average volume of tumors and weight of livers with xenografts were significantly decreased in NKX3.1-overexpressing mice (Fig. 2*E*). Meanwhile, the tissues of xenograft overexpressing NKX3.1 still maintained a high expression level of NKX3.1 (Fig. 2*E*). These results suggest that NKX3.1 represses cell proliferation *in vivo*, consistent with the *in vitro* results.

Overexpression of NKX3.1 suppresses HCC cells mobility in vitro and metastasis in vivo

Next, we explored the effect of NKX3.1 expression on HCC cells migration and invasion. The results of the *in vitro* wound-healing assay revealed NKX3.1 overexpression decreased migration of the HCC cells compared with the control (Fig. 3*A*). The *in vitro* invasion assay indicated that the invasive capacities of HCC cells were dramatically suppressed by NKX3.1 transfection compared with the control cells (Fig. 3*B*). To further investigate the role of NKX3.1 in HCC metastasis *in vivo*, paraffin sections were prepared with the liver tissues and lung tissues from the mice injected with HCC-LY10-pWPXL/NKX3.1 cells orthotopically, and histological examination was performed. The results showed that mice in the NKX3.1-overexpressing group exhibited fewer intrahepatic and lung metastasis nodules than the control mice (Fig. 3, *C* and *D*). In addition, all of the nine mice in the control group developed lung metastasis (100%), whereas only five of the nine mice in the NKX3.1-overexpressing group developed lung metastasis (55.56%). Collectively, these findings indicated that overexpression of NKX3.1 markedly inhibits the mobility of HCC cells *in vitro* and *in vivo*.

Knockdown of NKX3.1 promotes HCC cell proliferation and mobility in vitro

To determine the function of endogenous NKX3.1, three lentiviral vectors expressing effective shRNAs targeting *NKX3.1* were used to knock down endogenous NKX3.1 (Fig. 4*A*). As expected, knockdown of NKX3.1 in MHCC-97L markedly promoted cell growth and colony formation (Fig. 4, *B* and *C*). Results from the wound-healing assay (Fig. 4*D*) and *in vitro* invasion assay (Fig. 4*E*) showed that NKX3.1 down-regulation increased the cell migration and invasion capacities of MHCC-97L. The results validate the conclusions drawn by overexpression of NKX3.1.

Overexpression of NKX3.1 induces G_1/S phase arrest in HCC cells through up-regulation of FOXO1

To further investigate the inhibitory effect of NKX3.1 on HCC cell proliferation, the cell cycle distributions among SMMC-7721 and HCC-LY10 cells was evaluated by flow cytometry (Fig. 5*A*). After treatment of 2 mM thymidine for 24 h to synchronize cells at the G_1/S phase border, cells were collected at 0, 12, and 24 h. Flow cytometry analysis showed that the percentage of cells at the G_1 phase was significantly higher in the SMMC-7721–NKX3.1 and HCC-LY10–NKX3.1 cells than the control cells after the thymidine treatment (Fig. 5*B* and Table 1). Cells synchronized at the G_2/M phase boundary with 0.3 μM nocodazole displayed similar results (supplemental Fig. S2 and supplemental Table S6). We next detected the expression of essential molecules that regulate the G_1/S phase transition in NKX3.1-overexpressing cells and control cells. Upon NKX3.1 overexpression, protein levels of FOXO1 and its downstream molecules $p21^{CIP1}$ and $p27^{KIP1}$ increased notably, whereas protein levels of CDK2, Cyclin E, and phosphorylated RB (Ser-807/811) decreased (Fig. 5*C*). We then detected these proteins after treatment of thymidine for 0 and 24 h. As time goes on, expression of FOXO1, $p21^{CIP1}$, and $p27^{KIP1}$ increased in NKX3.1-overexpressing cells at 24 h, whereas expression of CDK2, Cyclin E, and phosphorylated RB (Ser-807/811) were decreased compared with control pWPXL cells (Fig. 5*D*). This implied that overexpression of NKX3.1 results in G_1/S phase arrest through up-regulating FOXO1 in HCC cells.

FOXO1 is a direct target of NKX3.1

Given the results that FOXO1 expression was up-regulated in NKX3.1 overexpression HCC cells, we then explored whether *FOXO1* is the direct target of NKX3.1. The JASPAR (jaspar.genereg.net)[4] database was used to analyze the potential NKX3.1-binding site in the *FOXO1* promoter (Fig. 6*A*). The promoter of the *FOXO1* gene, which spans a 1794-bp sequence upstream of the first ATG, was cloned and linked to pGL3 vector. The results of the luciferase assay showed that relative luciferase activity of the *FOXO1* promoter was significantly induced by overexpression of NKX3.1 (Fig. 6*B*). We then deleted the sequences that span the region from −1010 and −550 bp to the first ATG relative to the enhanced luciferase activity markedly in −550 bp (Fig. 6*C*). According to the sequence logo of the NKX3.1 potential binding site in JASPAR (jaspar.genereg.net)[4] we mutated the high-score base to the low-score base at the predicted NKX3.1-binding site (−230 to −239 bp), as shown in Fig. 6*D*. Enhanced luciferase activity was reversed by transfection of the mutant (Fig. 6*E*). Chromatin immunoprecipitation assay further verified that the site was the NKX3.1-binding site on the *FOXO1* promoter (Fig. 6*F*). Taken together, *FOXO1* promoter is a direct transcriptional target of NKX3.1.

[4] Please note that the JBC is not responsible for the long-term archiving and maintenance of this site or any other third party hosted site.

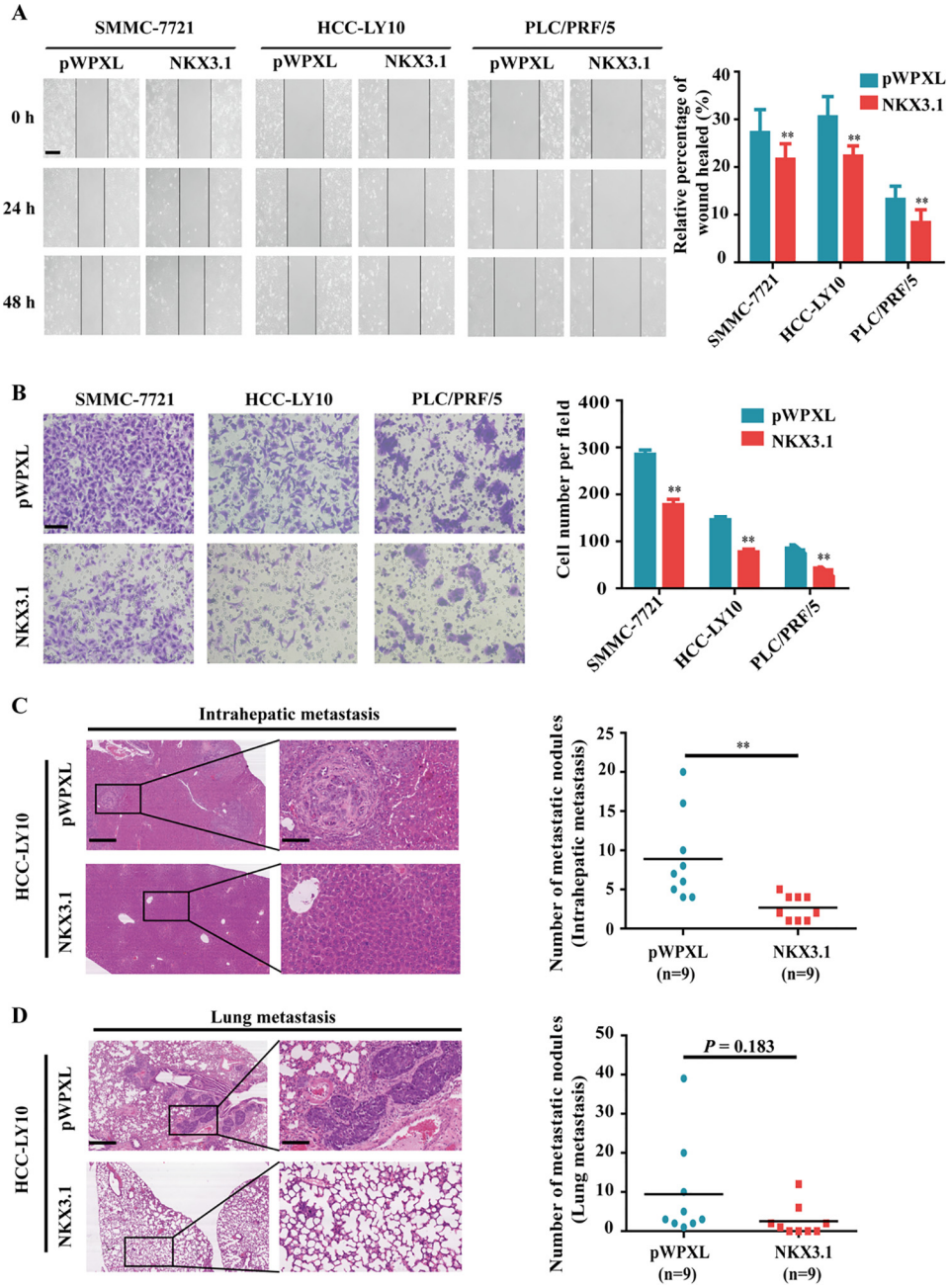

Figure 3. Overexpression of NKX3.1 suppresses HCC cell mobility *in vitro* and metastasis *in vivo*. *A,* overexpression of NKX3.1 suppressed HCC cell migration *in vitro* by wound healing assay. Original magnification: ×100; *scale bar*, 200 μm. The *bar graph* shows quantitative analysis data with three replicates. *B,* overexpression of NKX3.1 suppressed HCC cell invasion *in vitro*. Original magnification: ×200; *scale bar*, 100 μm. The *bar graph* shows quantitative analysis data with three replicates. *C, left panel* showed the representative images of intrahepatic metastatic nodules formed by HCC-LY10 cells transfected with *NKX3.1* or the control (original magnification: *left images*, ×40, *scale bar*, 500 μm; *right images*, ×200, *scale bar*, 100 μm). The *numbers* of intrahepatic metastatic nodules were presented in the *right panel* ($n = 9$). *D, left panel* showed representative images of lung metastatic nodules formed by the same cells in *C*. Original magnification: *left images*, ×40, and *scale bar*, 500 μm; *right images*, ×200, *scale bar*, 100 μm. The *right panel* presents the numbers of lung metastatic nodules ($n = 9$). **, $p < 0.01$.

FOXO1 is involved in the NKX3.1-induced suppressive effect of HCC cells

To explore whether FOXO1 up-regulation by NKX3.1 is responsible for the tumor suppressive function in HCC, FOXO1 expression was knocked down in SMMC-7721, HCC-LY10, and PLC/PRF/5 cells with stable overexpression of NKX3.1 (Fig. 7*A*). We use two lentiviral vectors expressing effective short hairpin RNAs designed to knock down FOXO1 (shFOXO1-1 and shFOXO1-2). We also tested the expression changes of cell cycle-related proteins (FOXO1, $p21^{CIP1}$, $p27^{KIP1}$, CDK2, Cyclin E, phosphorylated RB, and total RB) in NKX3.1-overexpressing HCC cells after knockdown of FOXO1. Upon FOXO1 knockdown, expression levels of $p21^{CIP1}$ and $p27^{KIP1}$ decreased, whereas expression levels of CDK2, Cyclin E, and phosphorylated RB increased. Thus, FOXO1 knockdown can rescue the NKX3.1 overexpression induced by the expression changes of cell cycle-related proteins. MTT and colony assays *in vitro* revealed that the decrease of FOXO1 significantly reversed NKX3.1-induced inhibition of cell proliferation (Fig. 7, *B* and *C*). Moreover,

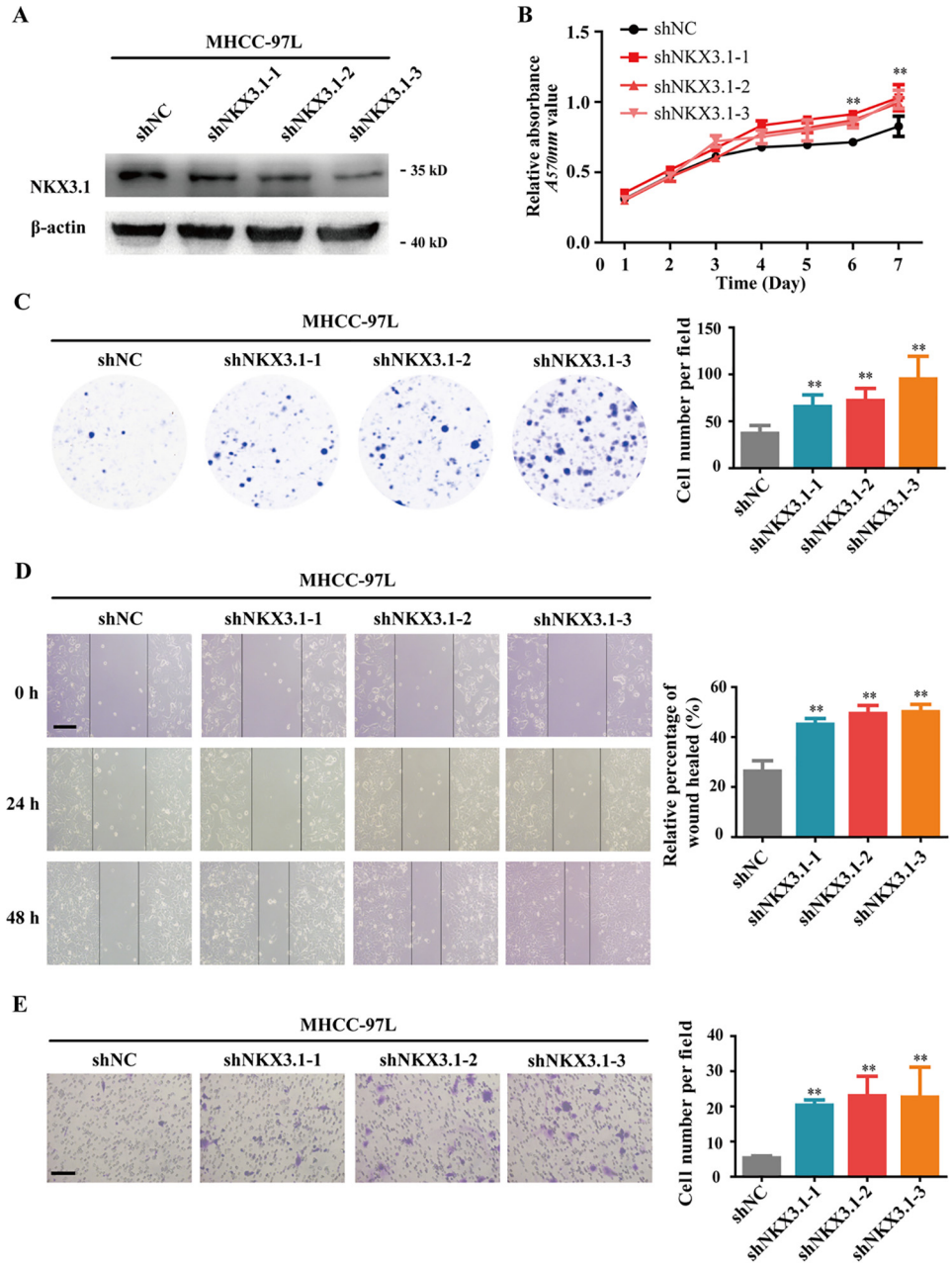

Figure 4. Knockdown of *NKX3.1* promotes HCC cell proliferation and mobility *in vitro*. *A,* Western blot analysis of NKX3.1 protein in MHCC-97L cell stably transfected with shNKX3.1 or negative control (*shNC*) vectors. *B,* knockdown of *NKX3.1* promoted the proliferation of MHCC-97L cell by MTT assay. *C,* knockdown of NKX3.1 increased the colony formation ability of HCC cell. The *bar graph* shows quantitative analysis data with three replicates. *D,* knockdown of *NKX3.1* increased HCC cell migration *in vitro* by wound-healing assay. Original magnification: ×100; *scale bar*, 200 μm. The *bar graph* shows the quantitative analysis data with three replicates. *E,* knockdown of *NKX3.1* promoted HCC cell invasion *in vitro*. Original magnification: ×200; *scale bar*, 100 μm. The *bar graph* shows the quantitative analysis data with three replicates. **, $p < 0.01$.

the inhibited invasion ability by NKX3.1 was reversed after FOXO1 interference (supplemental Fig. S3). Therefore, these data demonstrated that FOXO1 is a direct and functional target for NKX3.1 and is also responsible for the suppressive effects of NKX3.1 in HCC cells.

The expression levels of NKX3.1 and FOXO1 show positive correlation in HCC tissues

To further investigate the correlation between expression levels of *NKX3.1* and *FOXO1* in human primary HCC tissues, we detected *FOXO1* mRNA expression levels in 60 pairs of HCC tissues and matched adjacent noncancerous liver tissues and protein expression levels in 20 pairs of matched HCC/noncancerous liver tissues. *FOXO1* mRNA expression was down-regulated significantly in HCC tissues compared with noncancerous liver tissues (supplemental Fig. S4*A*). The result was in common with the analysis in TCGA cohort (supplemental Fig. S4*B*). Moreover, protein expression of FOXO1 was frequently down-regulated in HCC tissues (supplemental Fig. S4*C*). Analysis of the relative protein expression levels (tumor/non-tumor) of NKX3.1 and FOXO1 together showed that there was a positive correlation between NKX3.1 and FOXO1 protein

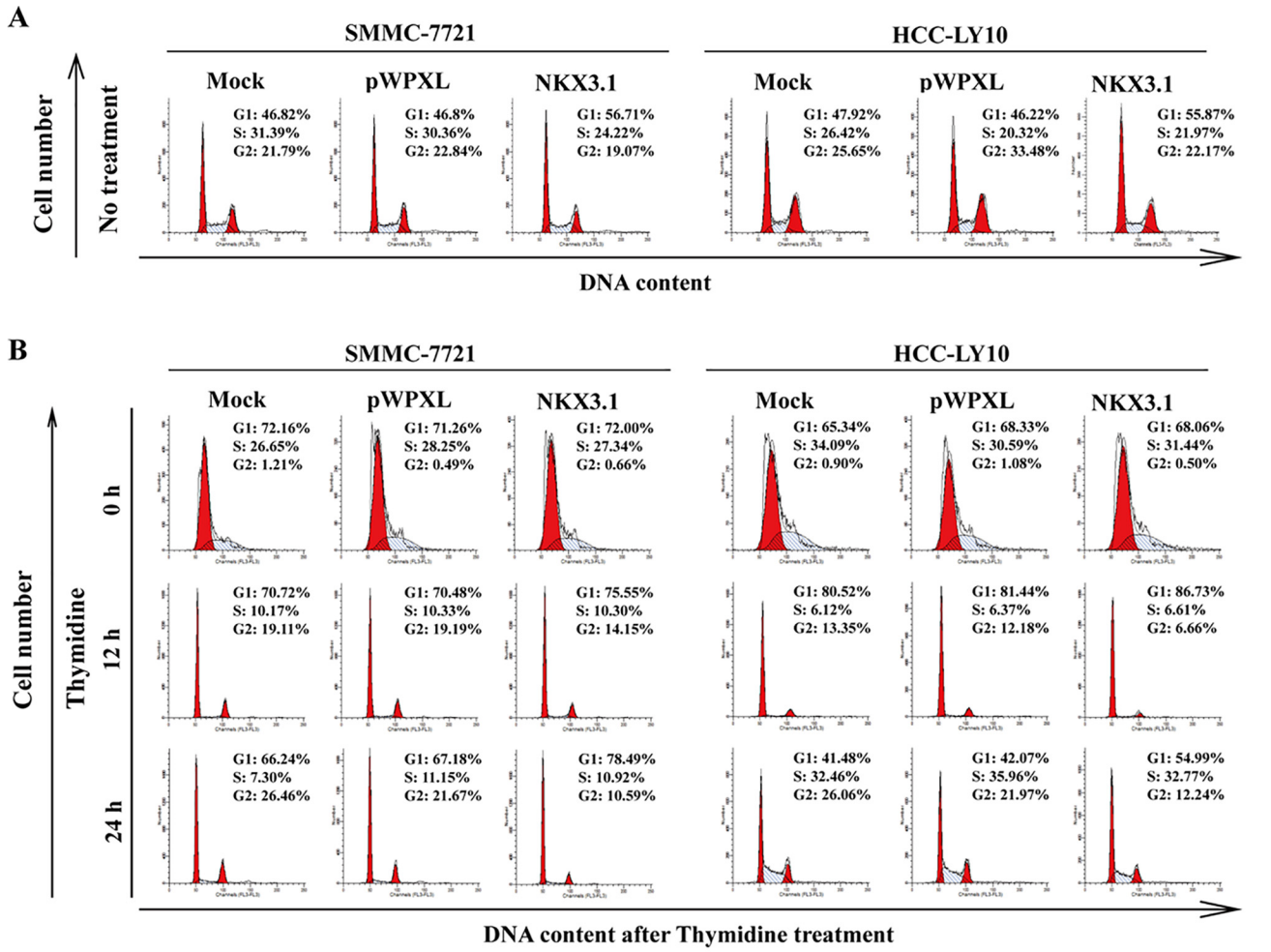
A
SMMC-7721
HCC-LY10
Mock
pWPXL
NKX3.1
Cell number
No treatment
G1: 46.82%
S: 31.39%
G2: 21.79%
G1: 46.8%
S: 30.36%
G2: 22.84%
G1: 56.71%
S: 24.22%
G2: 19.07%
G1: 47.92%
S: 26.42%
G2: 25.65%
G1: 46.22%
S: 20.32%
G2: 33.48%
G1: 55.87%
S: 21.97%
G2: 22.17%
DNA content
B
SMMC-7721
HCC-LY10
Mock
pWPXL
NKX3.1
Cell number
Thymidine
0 h
12 h
24 h
G1: 72.16%
S: 26.65%
G2: 1.21%
G1: 71.26%
S: 28.25%
G2: 0.49%
G1: 72.00%
S: 27.34%
G2: 0.66%
G1: 65.34%
S: 34.09%
G2: 0.90%
G1: 68.33%
S: 30.59%
G2: 1.08%
G1: 68.06%
S: 31.44%
G2: 0.50%
G1: 70.72%
S: 10.17%
G2: 19.11%
G1: 70.48%
S: 10.33%
G2: 19.19%
G1: 75.55%
S: 10.30%
G2: 14.15%
G1: 80.52%
S: 6.12%
G2: 13.35%
G1: 81.44%
S: 6.37%
G2: 12.18%
G1: 86.73%
S: 6.61%
G2: 6.66%
G1: 66.24%
S: 7.30%
G2: 26.46%
G1: 67.18%
S: 11.15%
G2: 21.67%
G1: 78.49%
S: 10.92%
G2: 10.59%
G1: 41.48%
S: 32.46%
G2: 26.06%
G1: 42.07%
S: 35.96%
G2: 21.97%
G1: 54.99%
S: 32.77%
G2: 12.24%
DNA content after Thymidine treatment
C
SMMC-7721
HCC-LY10
pWPXL
NKX3.1
NKX3.1
FOXO1
p21
p27
CDK2
Cyclin E
p-Rb
(Ser 807/811)
Rb
β-actin
D
Thymidine treatment
0 h
24 h
Mock
pWPXL
NKX3.1
35 kD
70 kD
20 kD
25 kD
35 kD
55 kD
100 kD
100 kD
40 kD
SMMC-7721
HCC-LY10

Table 1
The cell cycle distribution of SMMC-7721 and HCC-LY10 cells without transfection (mock) and those that were transfected with *NKX3.1* or control (*pWPXL*) vectors
Data are mean ± S.D. of three independent experiments.

Time		Cell cycle	SMMC-7721 (%)			HCC-LY10 (%)		
			Mock	*pWPXL*	*NKX3.1*	Mock	*pWPXL*	*NKX3.1*
No treatment		G_1	48.01 ± 0.6	45.94 ± 0.54	54.73 ± 2.22[a]	47.12 ± 0.38	47.28 ± 0.70	55.4 ± 1.32[a]
		S	24.56 ± 1.63	20.54 ± 0.67	22.04 ± 0.31	30.76 ± 0.68	29.79 ± 0.69	25.15 ± 1.39
		G_2/M	27.42 ± 1.57	33.52 ± 1.13	23.24 ± 1.93	22.12 ± 0.31	22.93 ± 0.11	19.45 ± 0.56
Synchronization with thymidine								
	0 h	G_1	72.16 ± 2.08	71.26 ± 1.15	72.00 ± 1.21	65.34 ± 1.09	68.33 ± 1.64	68.06 ± 0.93
		S	26.65 ± 2.59	28.25 ± 1.22	27.34 ± 1.24	34.09 ± 0.74	30.59 ± 1.60	31.44 ± 1.21
		G_2/M	1.21 ± 0.51	0.49 ± 0.14	0.66 ± 0.20	0.90 ± 0.34	1.08 ± 0.49	0.50 ± 0.32
	12 h	G_1	70.72 ± 0.65	70.48 ± 1.25	75.55 ± 0.32[a]	80.52 ± 0.45	81.44 ± 0.83	86.73 ± 0.29[a]
		S	10.17 ± 0.85	10.33 ± 0.92	10.30 ± 0.22	6.12 ± 0.19	6.37 ± 1.12	6.61 ± 0.43
		G_2/M	19.11 ± 1.29	19.19 ± 1.66	14.15 ± 0.53	13.35 ± 0.37	12.18 ± 0.31	6.66 ± 0.66
	24 h	G_1	66.24 ± 0.40	67.18 ± 0.76	78.49 ± 0.21[a]	41.48 ± 0.31	42.07 ± 0.67	54.99 ± 0.38[a]
		S	7.30 ± 0.43	11.15 ± 0.48	10.92 ± 0.14	32.46 ± 0.12	35.96 ± 0.60	32.77 ± 0.82
		G_2/M	26.46 ± 0.57	21.67 ± 0.29	10.59 ± 0.70	26.06 ± 0.22	21.97 ± 0.37	12.24 ± 0.87

[a] $p < 0.05$, comparing to the control pWPXL group.

expression in HCC and matched noncancerous liver tissues ($r = 0.677$, $p = 0.001$; Fig. 8, *A–D*). Of note, *FOXO1* mRNA expression was also positively associated with *NKX3.1* expression in HCC tissues (Fig. 8, *E* and *F*). In addition, we measured mRNA and protein expression levels of *FOXO1* in tissue samples of xenografts mentioned in Fig. 3*E*. FOXO1 is expressed highly in NKX3.1-overexpressing samples (supplemental Fig. S5, *A* and *B*). Taken together, these results suggest that the expression levels of NKX3.1 and FOXO1 show positive correlation in HCC tissues and are promising prognostic indicators for HCC patients in the clinic.

Discussion

NKX3.1 plays an important role in prostate development, proliferation of the prostate glandular epithelium, formation of prostatic ducts, and regulation of prostate epithelial differentiation (8, 9). NKX3.1 expression in androgen-deprived prostate epithelial marks a luminal cell population that appears as stem properties during prostate regeneration (24). Numerous reports have shown that *NKX3.1* acts as a tumor suppressor in prostate. Mouse models suggest that the phosphatase and tensin homolog deleted on chromosome 10 (*Pten*) loss could drive invasion and metastasis in cooperation with loss of *Nkx3.1* (11, 25). Moreover, loss of *NKX3.1* expression is strongly related to the advanced tumor stage in prostate cancer (26). It has been reported that the loss of NKX3.1 protein is mediated by several mechanisms, including gene methylation, post-translational modification, and genetic loss (27). Inflammation that releases cytokine TNF-α and IL1-β could destabilize the NKX3.1 protein by phosphorylating at serine 196 and decreasing its half-life (28). Phosphorylation at serine 185 is associated with ubiquitination signaling and degradation of the NKX3.1 protein in the proteasome (29). Song and colleagues (30) identified DYRK1B kinase as a target for enzymatic inhibition to increase cellular NKX3.1 expression in the prostate. Thus, searching for potential candidate targets mediated by the enhancing NKX3.1 expression level in HCC is meaningful for treatment.

However, the function and the role of NKX3.1 in other cancers were rarely reported. In the current study, we found that NKX3.1 was overexpressed in noncancerous liver tissues compared with HCC tissues. Analysis of the relationship between *NKX3.1* expression level and clinicopathological features in the TCGA cohort revealed that lower expression levels of *NKX3.1* are related to the malignant progression of HCC. These results suggest that NKX3.1 may play a negative regulating role in HCC progression. For the reason that endogenous NKX3.1 expression was at a low level, its stable overexpression cell lines were established to explore the function of NKX3.1 in HCC. We conformed for the first time that NKX3.1 suppresses HCC cell proliferation and metastasis *in vitro* and *in vivo*. Knockdown of NKX3.1 was also performed to validate the function of NKX3.1 in HCC.

Based on previous documents, *FOXO1* acts as a tumor suppressor in HCC, the underlying molecular mechanism of the anticancer effects of FOXO1 has been widely reported as well (31–35). Deletion of Aurora A kinase up-regulated FOXO1 in a p53-dependent manner and induces cell cycle arrest at the G_2/M phase (36). FOXO1 is downstream of the PI3K-Akt signaling. AQP9 overexpression in liver cancer cells inhibits PI3K/Akt signaling and subsequently increased FOXO1 protein expression, resulting in cell cycle arrest and apoptosis (37). However, the relationship between NKX3.1 and FOXO1 is still unknown in HCC. The data presented in our study showed that overexpression of NKX3.1 up-regulates expression of FOXO1 and p21, resulting in cell cycle arrest at the G_1/S phase. We report that NKX3.1 inhibits the HCC progression by up-regulating FOXO1 expression via directly binding to the promoter of *FOXO1*. In terms of invasion, we found that inhibited invasion by NKX3.1 could be reversed after FOXO1 interference. NKX3.1 could suppress cell invasion via FOXO1. There are

Figure 5. Overexpression of NKX3.1 induces cell cycle arrest at the G_1/S phase through up-regulation of FOXO1. *A,* the cell cycle distribution of SMMC-7721 and HCC-LY10 cells without transfection (*Mock*) and those that were transfected with *NKX3.1* or control (*pWPXL*) vectors. *B,* the cell cycle distribution of SMMC-7721 and HCC-LY10 cells (Mock/pWPXL/NKX3.1) collected at 0, 12, and 24 h after synchronizing with 2 mM thymidine. *C,* Western blot analysis of FOXO1, P21, P27, CDK2, Cyclin E, RB, phospho-RB (Ser-807/811) in NKX3.1-overexpressing SMMC-7721 and HCC-LY10 cells. *D,* Western blot analysis of the expressions of FOXO1, P21, P27, CDK2, Cyclin E, RB, phospho-Rb (Ser-807/811) in SMMC-7721 and HCC-LY10 cells (Mock/pWPXL/NKX3.1) collected at 0 and 24 h after synchronizing with 2 mM thymidine. β-Actin was used as a loading control.

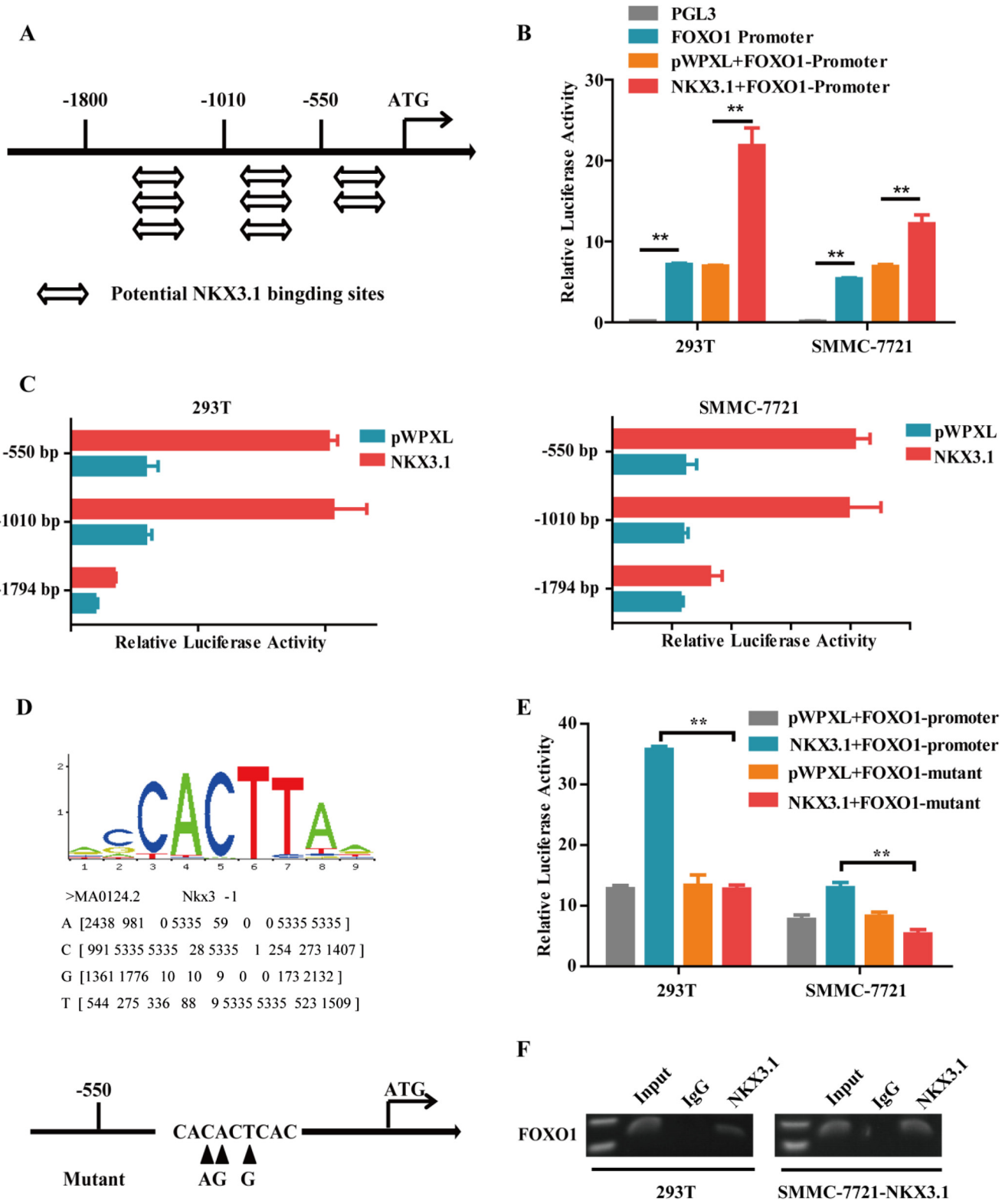

Figure 6. NKX3.1 up-regulates *FOXO1* expression through directly binding to FOXO1 promoter. *A,* potential NKX3.1-binding sites in the *FOXO1* promoter identified with the JASPAR database (http://jaspar.genereg.net/).[4] *B,* relative activities of the *FOXO1* promoter after transfection of NKX3.1 and pWPXL into HEK 293T and SMMC-7721 cells analyzed by luciferase assay. *C,* relative activities of *FOXO1* promoter deletion mutants in HEK 293T and SMMC-7721 cells by luciferase assay. *D,* the *top panel* is the sequence logo of NKX3.1 potential binding site in JASPAR (http://jaspar.genereg.net/).[4] The *bottom panel* is the diagram of mutant sites in the *FOXO1* promoter. *E,* relative activities of the *FOXO1* promoter and the mutant promoter after transfection of NKX3.1 and pWPXL. Data are mean ± S.D. from experiments with three replicates. **, $p < 0.01$. *F,* binding of NKX3.1 to the *FOXO1* promoter was performed by ChIP using the antibody against NKX3.1 and negative control (IgG) in 293T and NKX3.1-overexpressing SMMC-7721 cells.

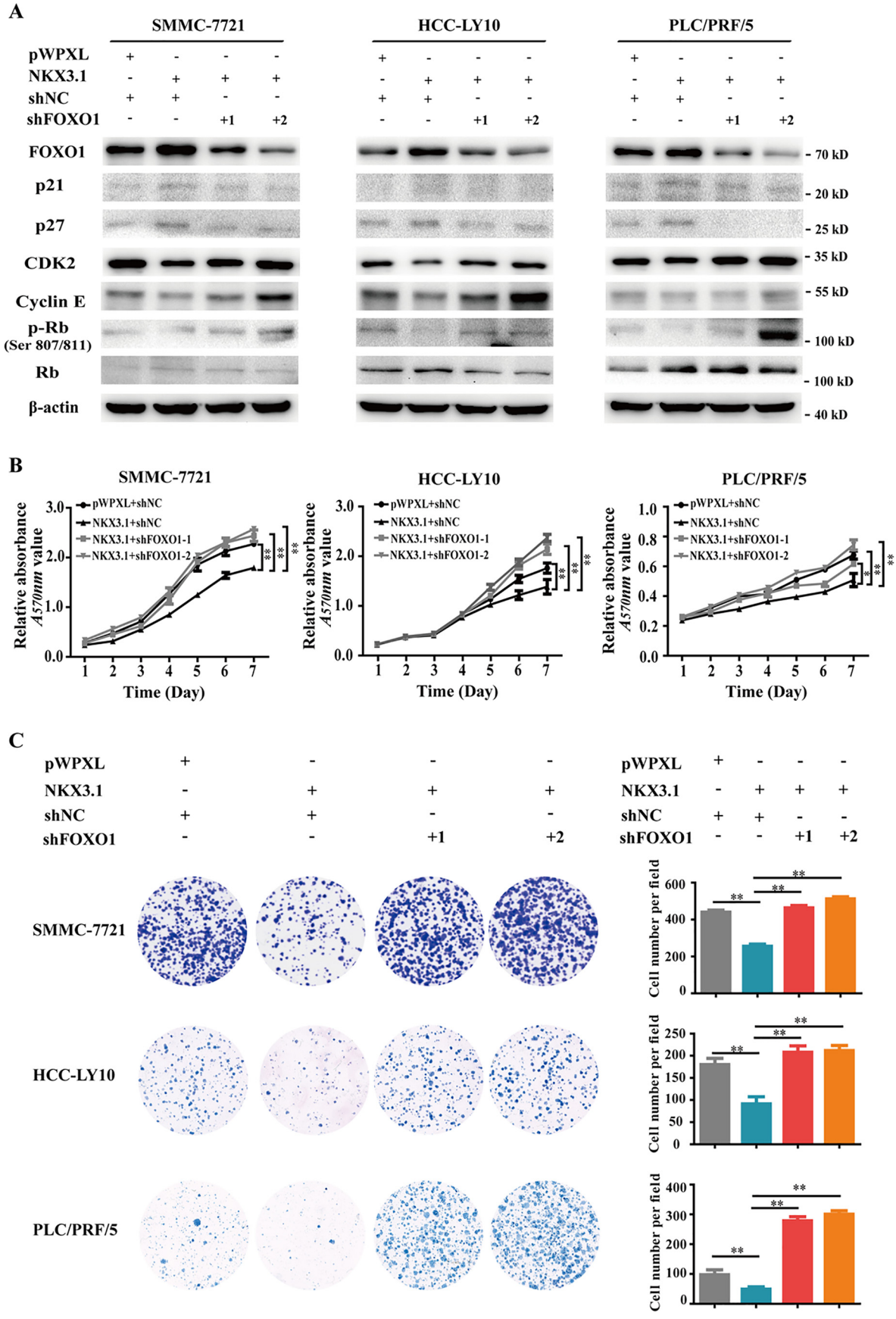
A
SMMC-7721
HCC-LY10
PLC/PRF/5
pWPXL
NKX3.1
shNC
shFOXO1
FOXO1
p21
p27
CDK2
Cyclin E
p-Rb (Ser 807/811)
Rb
β-actin
70 kD
20 kD
25 kD
35 kD
55 kD
100 kD
100 kD
40 kD
B
SMMC-7721
HCC-LY10
PLC/PRF/5
pWPXL+shNC
NKX3.1+shNC
NKX3.1+shFOXO1-1
NKX3.1+shFOXO1-2
Relative absorbance A570nm value
Time (Day)
C
SMMC-7721
HCC-LY10
PLC/PRF/5
Cell number per field

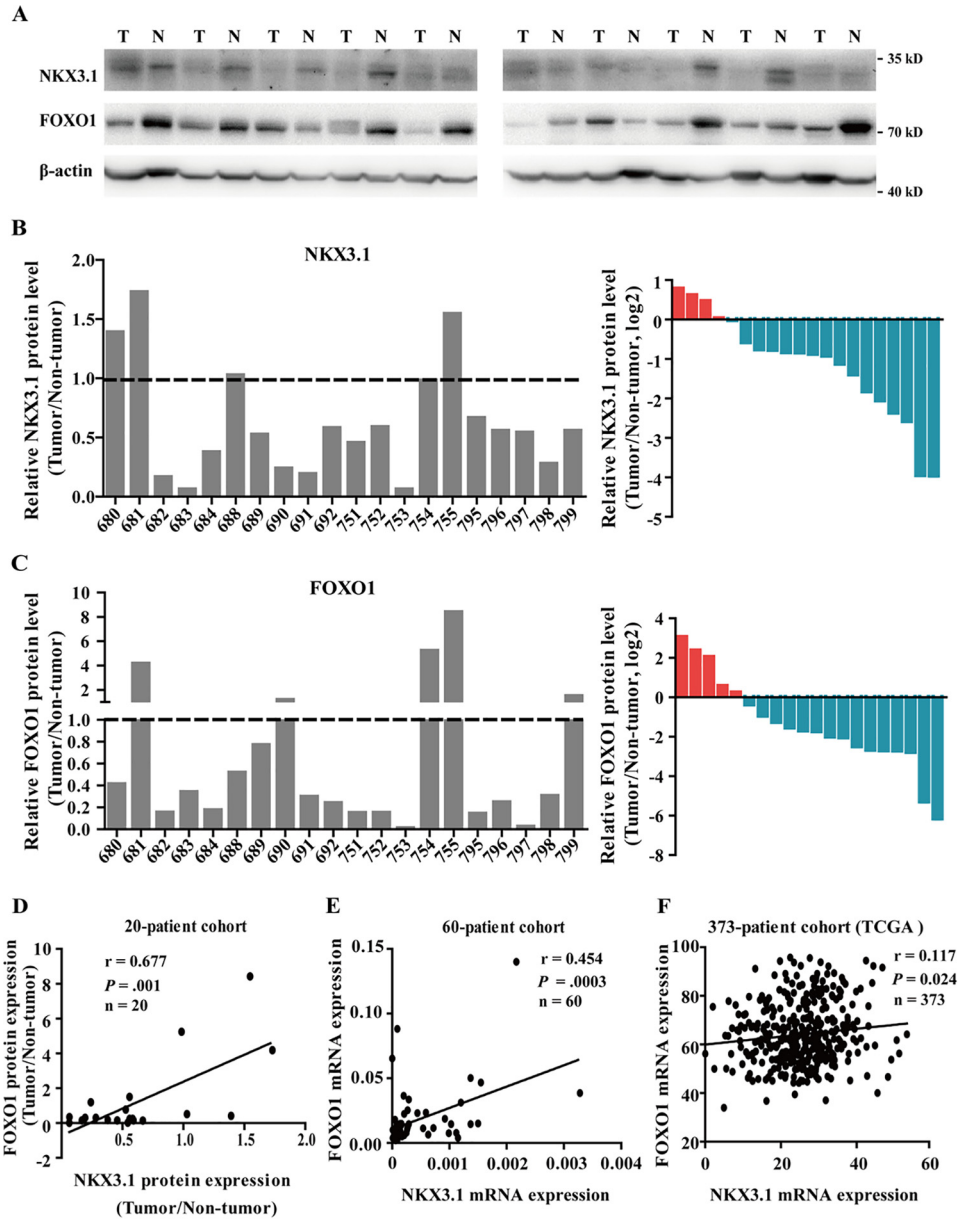

Figure 8. Positive correlation between FOXO1 and NKX3.1 expression in human HCC tissues. *A,* representative images of NKX3.1 and FOXO1 protein levels in human HCC tissues (*T*) and the corresponding adjacent non-cancerous liver tissues (*N*). β-Actin was used as a loading control. Images were taken from Fig. 1*C* and supplemental Fig. S4C. *B* and *C,* the fold-change of *NKX3.1* (*B*) and *FOXO1* (*C*) protein levels in 20 paired HCC/non-cancerous liver tissues. Data were normalized to β-actin and presented as $\log_2$ fold-change. *Red bar* in the waterfall plot represents a patient with a higher expression of *NKX3.1* or *FOXO1* in HCC tissues than paired non-cancerous liver tissue; the *gray bar* represents a patient with a lower expression of *NKX3.1* or *FOXO1* in HCC tissues than paired non-cancerous liver tissue. *D,* the correlation between NKX3.1 and FOXO1 protein levels in 20 paired HCC/non-cancerous liver tissues. *E* and *F,* the correlation between *NKX3.1* and *FOXO1* mRNA levels in HCC tissues of 60 patients (*E*) and 373 patient TCGA cohort (*F*). The Pearson correlation coefficients (*r*) and *p* value were indicated.

studies reported that FOXO1 inhibits cell migration and invasion in HCC and prostate cancer as well (38–40). In HCC, FOXO1 expression levels are inversely correlated with epithelial-to-mesenchymal transition inducers and it directly inhibits ZEB2 expression to suppress epithelial-to-mesenchymal transition (41). It is worthy to explore whether NKX3.1 suppresses cell invasion and metastasis through inhibiting epithelial-to-mesenchymal transition in HCC.

NKX3.1 exerts tumor suppressive effects in prostate cancer partly by activating the cellular response to oxidation and accelerating DNA repair. It is reported that NKX3.1 has an important role in regulating the DNA damage response by interacting with ataxia telangiectasia-mutated kinase and by activation of topoisomerase I (16, 42–44). Early molecular events in prostate cancer often include gene rearrangement of *ETS* family members and loss of *NKX3.1* expression (45). Bowen and colleagues

Figure 7. Knockdown of *FOXO1* after NKX3.1 overexpression rescues NKX3.1-induced suppressive effect of HCC cells. *A,* Western blot analysis of expression levels of FOXO1 and cell cycle-related proteins shown in Fig. 4 in NKX3.1-overexpressing HCC cells after knockdown of FOXO1. β-Actin was used as a loading control. *B,* knockdown of *FOXO1* reversed the inhibitory effect of *NKX3.1* on cell proliferation *in vitro* by MTT assay. *C,* knockdown of *FOXO1* reversed the inhibitory effect of *NKX3.1* on cell colony formation *in vitro*. Data are mean ± S.D. from experiments with three replicates. *, $p < 0.05$; **, $p < 0.01$.

(46) showed that NKX3.1 protein loss that occurs in intraepithelial neoplasia and prostate inflammation predisposes to the *ETS* gene rearrangement including *TMPRSS2* and *EGR*. NKX3.1 influences the recruitment of the proteins that promote DNA repair. Further studies are needed to explore whether NKX3.1 is responsible for DNA damage repair in HCC.

In conclusion, our findings demonstrate that NKX3.1 suppresses HCC cell proliferation through regulating the expression of FOXO1 and inducing cell cycle arrest at G_1/S phase. In addition, NKX3.1 significantly inhibits migration, invasion, and metastasis of HCC cells *in vitro* and *in vivo*. These data suggest that NKX3.1 may serve as a promising therapeutic target for HCC treatment.

Experimental procedures

Human liver specimens and TCGA cohort

Sixty paired human primary HCC/matched adjacent noncancerous liver tissue specimens were obtained from Qidong Liver Cancer Institute. Informed consent was obtained from all patients, and the collection of tissue specimens for clinical analysis was approved by the University Ethical Committee. TCGA data were accessed from the website (https://tcga-data.nci.nih.gov/tcga/).[4] We downloaded LIHC gene expression (Illumina-HiSeq percentile) data including all of the 373 liver cancer patients (mRNA expression data of 50 paired cancer/noncancerous tissues were available) to analyze the mRNA expression levels of *NKX3.1* and *FOXO1*. The tests were performed on matched samples.

Cell lines and culture

The human hepatocellular carcinoma cell lines SMMC-7721 and Li7 were purchased from the cell bank of the Institute of Biochemistry and Cell Biology of the Chinese Academy of Sciences (Shanghai, China). Huh7 cells were obtained from the Riken Cell Bank. MHCC-LM3 and MHCC-97L cells were kindly provided by the Liver Cancer Institute of Zhongshan Hospital at Fudan University (Shanghai, China). The HCC-LY10 cell line was established in our laboratory. The PLC/PRF/5 and SK-Hep1 cell lines, immortalized normal hepatocyte L02, and human embryonic kidney 293T cell line were obtained from the American Type Culture Collection (Manassas, VA). All cells were cultured in Dulbecco's modified Eagle's medium (DMEM, Gibco). The medium contained 10% fetal bovine serum (FBS, Gibco), 100 μg/ml of streptomycin, and 100 units/ml of penicillin (Sigma) in a humidified 37 °C incubator with 5% CO_2.

Quantitative real-time polymerase chain reaction (qRT-PCR)

Total RNA from human primary HCC tissues and cell lines were extracted using TRIzol reagent (Invitrogen). Complementary DNA from reverse transcription was performed using the PrimeScript™ RT Reagent Kit (TaKaRa Bio, Japan). The real-time PCR using SYBR Green Master Mix (TaKaRa Bio, Japan) was performed with an Applied Biosystems 7500 Software version 2.0.5 real-time PCR system (Thermo Scientific). The primer sequences are listed in supplemental Table S1. The expression data were normalized to the mean of the housekeeping gene *GAPDH*.

Western blotting

Proteins extracted from HCC tissues and cells were lysed by RIPA buffer (Thermo Scientific) containing protease inhibitor mixture and phosphatase inhibitor (Roche, Welwyn Garden, Swiss), separated by 10% SDS-PAGE, and transferred to 0.45-μm polyvinylidene difluoride membranes (Merck Millipore). After blocking with 5% nonfat milk solution for 1 h at room temperature, the membranes were incubated with primary antibody at 4 °C overnight and probed with HRP-conjugated secondary antibody for 1.5 h at room temperature. The antibody information is listed in supplemental Table S2.

Plasmid constructs, lentivirus production, and cell transfection

The full-length human *NKX3.1* open read frame cDNA sequence was generated and cloned into the lentiviral vector pWPXL (Addgene, Cambridge, MA). The *FOXO1* promoter, which spans a 1794-bp sequence upstream of the first ATG was amplified. The deleted sequences span the region from −1010 and −550 bp to the first ATG. The mutant was generated by mutating the DNA-binding site (−230 to −239 bp). All promoter sequences were cloned into the pGL3 vector (Promega, Madison, WI). The primers for cloning are provided in supplemental Table S3. shRNAs targeting *NKX3.1*, *FOXO1*, and a negative control (shNC) were obtained from Genechem (Shanghai, China). Target sequences are listed in supplemental Table S4. Lentivirus production and cell transfection were performed as described previously (47).

Cell proliferation assay (MTT assay)

A total of 1000 cells were seeded into 96-well culture plates per well and incubated for 7 days. MTT reagent (5 mg/ml, Sigma) was added to each well and incubated at 37 °C. After 4 h, the formazan was dissolved in 100 μl of DMSO and the absorbance value was measured at 570 nm. Each experiment was performed in triplicate.

In vitro plate colony formation assay

A total of 1000 cells were seeded into 6-well culture plates per well and cultured for 2 weeks. Then cells were washed with PBS twice and fixed in 10% neutral phosphate-buffered formalin for 30 min. Cells were stained with Giemsa (Sigma) for another 30 min at room temperature. Each experiment was performed in triplicate.

Flow cytometry analysis

The cell cycle distribution was detected using flow cytometry analysis. Cells were plated into 6-well culture plates at a density of 1×10^6 cells per well for 24 h. They were treated with 2 mM thymidine or 0.3 μM nocodazole (Sigma) for 24 h to be synchronized at the G_1/S and G_2/M boundaries. Cells were then harvested by trypsin after 0, 12, and 24 h, centrifuged, and washed with PBS twice and fixed with 70% ethanol at −20 °C overnight. Before analysis by flow cytometry, cells were washed twice again with PBS and resuspended with 400 mg/ml of propidium iodide, 10 mg/ml of RNase (Sigma), and 0.1% Triton X-100 in 500 μl of PBS at 4 °C for 30 min. DNA content was quantified using Modfit 3.2 software. Each experiment was performed in triplicate.

In vitro wound-healing assay

Cells were plated into 6-well culture plates equally and grow to about 90% confluence in 24 h. We used the fine end of a 200-μl pipette tip to create an artificial homogenous wound in the monolayer. After scratching, the cells were cultured in DMEM containing 2% FBS and 1 mM thymidine (Sigma). Before taking pictures, cells were washed twice with serum-free DMEM. Images of cells migrating into the wound were photographed at 0, 24, and 48 h using an inverted fluorescence microscope (Axiovert 200, HAL 100, Carl ZEISS, Oberkochen, Germany) under a $\times$10 objective lens. Each experiment was performed in triplicate.

In vitro invasion assay

A total of 1×10^5 cells were seeded into the top chamber of a transwell (BD Biosciences) in serum-free DMEM, whereas the bottom chamber was filled with DMEM containing 10% FBS. The transwell chambers contained Matrigel-coated membrane filter inserts. After 24 h incubation, cells adhering to the lower membrane of the inserts were fixed in 10% neutral phosphate-buffered formalin for 30 min, stained with Giemsa solution, and counted in five randomly selected fields.

Luciferase assay

Cells were plated in 96-well culture plates for 24 h and grown to about 90% confluence in 24 h. Cells were then transfected with the relevant reporter plasmids and the PRL-TK reporter construct with Lipofectamine 2000 (Invitrogen). Forty-eight hours later, firefly luciferase activity and *Renilla* activity were determined according to the manufacturer's instructions (Promega).

Chromatin immunoprecipitation (ChIP)

ChIP assay was performed in SMMC-7721–pWPXL and SMMC-7721–NKX3.1 cells. Cells were cross-linked with 10% formaldehyde and reversed with 1 M glycine. After washing with PBS buffer, cells were harvested in Tissue Protein Extraction Reagent (Thermo Scientific) for 5 min on ice and centrifuged at 2,000 $\times$ *g* for 5 min. The precipitants were suspended in nuclei lyses buffer and DNA was crushed into fragments by sonication. Mouse anti-NKX3.1 (Invitrogen) or mouse IgG with protein A/G-agarose beads (Sigma) were added and incubated overnight at 4 °C to immunoprecipitate DNA-containing complexes. After washing, DNA was isolated and used for PCR analysis. Primers for the *FOXO1* promoter were: forward, 5′-cactgagaaggcgagagaatc-3′ and reverse, 5′-ggttttccacggggaggc-3′.

Tumor xenograft models

Six to 8-week-old male NOD/SCID mice were divided into groups randomly. For the liver orthotropic model, 2×10^6 SMMC-7721 cells or HCC-LY10 cells stably expressing NKX3.1 and control pWPXL were suspended in serum-free DMEM with Matrigel (1:1, BD Biosciences) for each mouse. After 4 to 6 weeks, all mice were sacrificed. Xenograft tumors were weighted, collected livers and lungs were fixed in 10% neutral phosphate-buffered formalin. The samples were embedded in paraffin and stained with hematoxylin and eosin. All animal experimental protocols were approved by the Shanghai Medical Experimental Animal Care Commission.

Statistical analysis

The data were presented as the mean $\pm$ S.D. Statistical analysis (comparisons between two groups) was performed using Student's *t* test. The Pearson correlation was performed to analyze the correlation between expression levels of NKX3.1 and FOXO1. $p < 0.05$ was considered statistically significant (*, $p < 0.05$; **, $p < 0.01$). Statistical analyses were performed using SPSS (Statistical Package for the Social Sciences) 19.0 software and GraphPad Prism 5.

Author contributions—J. Y. J. and J. J. L. designed the study and analyzed the data. J. Y. J. and H. L. performed the *in vitro* function of NKX3.1-overexpression and molecular mechanism experiments. Z. L. performed the *in vitro* functional experiments of NKX3.1-knockdown. C. C. extracted the plasmids of shRNAs targeting *NKX3.1*. F. Y. Z. and M. Y. performed the *in vivo* experiments. C. G. performed the histopathological examination. T. Y. C collected the primary HCC tissue samples and clinical significant survey and analysis. J. Y. J. wrote the manuscript. All authors reviewed the results and approved the final version of the manuscript.

References

1. Siegel, R. L., Miller, K. D., and Jemal, A. (2017) Cancer statistics, 2017. *CA Cancer J. Clin.* **67,** 7–30
2. Critelli, R. M., De Maria, N., and Villa, E. (2015) Biology of hepatocellular carcinoma. *Dig. Dis.* **33,** 635–641
3. Ferlay, J., Soerjomataram, I., Dikshit, R., Eser, S., Mathers, C., Rebelo, M., Parkin, D. M., Forman, D., and Bray, F. (2015) Cancer incidence and mortality worldwide: sources, methods and major patterns in GLOBOCAN 2012. *Int. J. Cancer* **136,** E359–E386
4. Taylor, B. S., Schultz, N., Hieronymus, H., Gopalan, A., Xiao, Y., Carver, B. S., Arora, V. K., Kaushik, P., Cerami, E., Reva, B., Antipin, Y., Mitsiades, N., Landers, T., Dolgalev, I., Major, J. E., *et al.* (2010) Integrative genomic profiling of human prostate cancer. *Cancer Cell* **18,** 11–22
5. Kang, J. (2015) Genomic alterations on 8p21-p23 are the most frequent genetic events in stage I squamous cell carcinoma of the lung. *Exp. Ther. Med.* **9,** 345–350
6. Kurimoto, F., Gemma, A., Hosoya, Y., Seike, M., Takenaka, K., Uematsu, K., Yoshimura, A., Shibuya, M., and Kudoh, S. (2001) Unchanged frequency of loss of heterozygosity and size of the deleted region at 8p21–23 during metastasis of lung cancer. *Int. J. Mol. Med.* **8,** 89–93
7. He, W. W., Sciavolino, P. J., Wing, J., Augustus, M., Hudson, P., Meissner, P. S., Curtis, R. T., Shell, B. K., Bostwick, D. G., Tindall, D. J., Gelmann, E. P., Abate-Shen, C., and Carter, K. C. (1997) A novel human prostate-specific, androgen-regulated homeobox gene (NKX3.1) that maps to 8p21, a region frequently deleted in prostate cancer. *Genomics* **43,** 69–77
8. Bieberich, C. J., Fujita, K., He, W. W., and Jay, G. (1996) Prostate-specific and androgen-dependent expression of a novel homeobox gene. *J. Biol. Chem.* **271,** 31779–31782
9. Bhatia-Gaur, R., Donjacour, A. A., Sciavolino, P. J., Kim, M., Desai, N., Young, P., Norton, C. R., Gridley, T., Cardiff, R. D., Cunha, G. R., Abate-Shen, C., and Shen, M. M. (1999) Roles for Nkx3.1 in prostate development and cancer. *Genes Dev.* **13,** 966–977
10. Sciavolino, P. J., Abrams, E. W., Yang, L., Austenberg, L. P., Shen, M. M., and Abate-Shen, C. (1997) Tissue-specific expression of murine Nkx3.1 in the male urogenital system. *Dev. Dyn.* **209,** 127–138
11. Kim, M. J., Cardiff, R. D., Desai, N., Banach-Petrosky, W. A., Parsons, R., Shen, M. M., and Abate-Shen, C. (2002) Cooperativity of Nkx3.1 and Pten loss of function in a mouse model of prostate carcinogenesis. *Proc. Natl. Acad. Sci. U.S.A.* **99,** 2884–2889

12. Dutta, A., Le Magnen, C., Mitrofanova, A., Ouyang, X., Califano, A., and Abate-Shen, C. (2016) Identification of an NKX3.1-G9a-UTY transcriptional regulatory network that controls prostate differentiation. *Science* **352,** 1576–1580
13. Kim, M. J., Bhatia-Gaur, R., Banach-Petrosky, W. A., Desai, N., Wang, Y., Hayward, S. W., Cunha, G. R., Cardiff, R. D., Shen, M. M., and Abate-Shen, C. (2002) Nkx3.1 mutant mice recapitulate early stages of prostate carcinogenesis. *Cancer Res.* **62,** 2999–3004
14. Debelec-Butuner, B., Alapinar, C., Ertunc, N., Gonen-Korkmaz, C., Yörükoğlu, K., and Korkmaz, K. S. (2014) TNFalpha-mediated loss of β-catenin/E-cadherin association and subsequent increase in cell migration is partially restored by NKX3.1 expression in prostate cells. *PLoS ONE* **9,** e109868
15. Tomlins, S. A., Rhodes, D. R., Perner, S., Dhanasekaran, S. M., Mehra, R., Sun, X. W., Varambally, S., Cao, X., Tchinda, J., Kuefer, R., Lee, C., Montie, J. E., Shah, R. B., Pienta, K. J., Rubin, M. A., and Chinnaiyan, A. M. (2005) Recurrent fusion of TMPRSS2 and ETS transcription factor genes in prostate cancer. *Science* **310,** 644–648
16. Bowen, C., and Gelmann, E. P. (2010) NKX3.1 activates cellular response to DNA damage. *Cancer Res.* **70,** 3089–3097
17. Bhatt, S., Stender, J. D., Joshi, S., Wu, G., and Katzenellenbogen, B. S. (2016) OCT-4: a novel estrogen receptor-α collaborator that promotes tamoxifen resistance in breast cancer cells. *Oncogene* **35,** 5722–5734
18. Miyaguchi, K., Uzawa, N., Mogushi, K., Takahashi, K., Michikawa, C., Nakata, Y., Sumino, J., Okada, N., Mizushima, H., Fukuoka, Y., and Tanaka, H. (2012) Loss of NKX3–1 as a potential marker for an increased risk of occult lymph node metastasis and poor prognosis in oral squamous cell carcinoma. *Int. J. Oncol.* **40,** 1907–1914
19. Zhang, Y., Gan, B., Liu, D., and Paik, J. H. (2011) FoxO family members in cancer. *Cancer Biol. Ther.* **12,** 253–259
20. Yu, F., Jin, L., Yang, G., Ji, L., Wang, F., and Lu, Z. (2014) Post-transcriptional repression of FOXO1 by QKI results in low levels of FOXO1 expression in breast cancer cells. *Oncol. Rep.* **31,** 1459–1465
21. Fendler, A., Jung, M., Stephan, C., Erbersdobler, A., Jung, K., and Yousef, G. M. (2013) The antiapoptotic function of miR-96 in prostate cancer by inhibition of FOXO1. *PLoS ONE* **8,** e80807
22. Fan, C., Liu, S., Zhao, Y., Han, Y., Yang, L., Tao, G., Li, Q., and Zhang, L. (2013) Upregulation of miR-370 contributes to the progression of gastric carcinoma via suppression of FOXO1. *Biomed. Pharmacother.* **67,** 521–526
23. Calvisi, D. F., Ladu, S., Pinna, F., Frau, M., Tomasi, M. L., Sini, M., Simile, M. M., Bonelli, P., Muroni, M. R., Seddaiu, M. A., Lim, D. S., Feo, F., and Pascale, R. M. (2009) SKP2 and CKS1 promote degradation of cell cycle regulators and are associated with hepatocellular carcinoma prognosis. *Gastroenterology* **137,** 1816–1826.e1–10
24. Wang, X., Kruithof-de Julio, M., Economides, K. D., Walker, D., Yu, H., Halili, M. V., Hu, Y. P., Price, S. M., Abate-Shen, C., and Shen, M. M. (2009) A luminal epithelial stem cell that is a cell of origin for prostate cancer. *Nature* **461,** 495–500
25. Abate-Shen, C., Banach-Petrosky, W. A., Sun, X., Economides, K. D., Desai, N., Gregg, J. P., Borowsky, A. D., Cardiff, R. D., and Shen, M. M. (2003) Nkx3.1: Pten mutant mice develop invasive prostate adenocarcinoma and lymph node metastases. *Cancer Res.* **63,** 3886–3890
26. Bowen, C., Bubendorf, L., Voeller, H. J., Slack, R., Willi, N., Sauter, G., Gasser, T. C., Koivisto, P., Lack, E. E., Kononen, J., Kallioniemi, O. P., and Gelmann, E. P. (2000) Loss of NKX3.1 expression in human prostate cancers correlates with tumor progression. *Cancer Res.* **60,** 6111–6115
27. Asatiani, E., Huang, W. X., Wang, A., Rodriguez Ortner, E., Cavalli, L. R., Haddad, B. R., and Gelmann, E. P. (2005) Deletion, methylation, and expression of the NKX3.1 suppressor gene in primary human prostate cancer. *Cancer Res.* **65,** 1164–1173
28. Khalili, M., Mutton, L. N., Gurel, B., Hicks, J. L., De Marzo, A. M., and Bieberich, C. J. (2010) Loss of Nkx3.1 expression in bacterial prostatitis: a potential link between inflammation and neoplasia. *Am. J. Pathol.* **176,** 2259–2268
29. Markowski, M. C., Bowen, C., and Gelmann, E. P. (2008) Inflammatory cytokines induce phosphorylation and ubiquitination of prostate suppressor protein NKX3.1. *Cancer Res.* **68,** 6896–6901
30. Song, L. N., Silva, J., Koller, A., Rosenthal, A., Chen, E. I., and Gelmann, E. P. (2015) The tumor suppressor NKX3.1 is targeted for degradation by DYRK1B kinase. *Mol. Cancer Res.* **13,** 913–922
31. Tikhanovich, I., Cox, J., and Weinman, S. A. (2013) Forkhead box class O transcription factors in liver function and disease. *J. Gastroenterol. Hepatol.* **28, 1**25–131
32. Xu, D., He, X., Chang, Y., Xu, C., Jiang, X., Sun, S., and Lin, J. (2013) Inhibition of miR-96 expression reduces cell proliferation and clonogenicity of HepG2 hepatoma cells. *Oncol. Rep.* **29,** 653–661
33. Yamaguchi, F., Hirata, Y., Akram, H., Kamitori, K., Dong, Y., Sui, L., and Tokuda, M. (2013) FOXO/TXNIP pathway is involved in the suppression of hepatocellular carcinoma growth by glutamate antagonist MK-801. *BMC Cancer* **13,** 468
34. Jung, H. S., Seo, Y. R., Yang, Y. M., Koo, J. H., An, J., Lee, S. J., Kim, K. M., and Kim, S. G. (2014) Galpha12gep oncogene inhibits FOXO1 in hepatocellular carcinoma as a consequence of miR-135b and miR-194 dysregulation. *Cell. Signal.* **26,** 1456–1465
35. Yang, X. W., Shen, G. Z., Cao, L. Q., Jiang, X. F., Peng, H. P., Shen, G., Chen, D., and Xue, P. (2014) MicroRNA-1269 promotes proliferation in human hepatocellular carcinoma via downregulation of FOXO1. *BMC Cancer* **14,** 909
36. Lee, S. Y., Lee, G. R., Woo, D. H., Park, N. H., Cha, H. J., Moon, Y. H., and Han, I. S. (2013) Depletion of Aurora A leads to upregulation of FoxO1 to induce cell cycle arrest in hepatocellular carcinoma cells. *Cell Cycle* **12,** 67–75
37. Li, C. F., Zhang, W. G., Liu, M., Qiu, L. W., Chen, X. F., Lv, L., and Mei, Z. C. (2016) Aquaporin 9 inhibits hepatocellular carcinoma through upregulating FOXO1 expression. *Oncotarget* **7,** 44161–44170
38. Zhang, H., Pan, Y., Zheng, L., Choe, C., Lindgren, B., Jensen, E. D., Westendorf, J. J., Cheng, L., and Huang, H. (2011) FOXO1 inhibits Runx2 transcriptional activity and prostate cancer cell migration and invasion. *Cancer Res.* **71,** 3257–3267
39. Wallis, C. J., Gordanpour, A., Bendavid, J. S., Sugar, L., Nam, R. K., and Seth, A. (2015) MiR-182 Is Associated with Growth, Migration and Invasion in Prostate Cancer via Suppression of FOXO1. *J. Cancer* **6,** 1295–1305
40. Zeng, Y. B., Liang, X. H., Zhang, G. X., Jiang, N., Zhang, T., Huang, J. Y., Zhang, L., and Zeng, X. C. (2016) miRNA-135a promotes hepatocellular carcinoma cell migration and invasion by targeting forkhead box O1. *Cancer Cell Int.* **16,** 63
41. Dong, T., Zhang, Y., Chen, Y., Liu, P., An, T., Zhang, J., Yang, H., Zhu, W., and Yang, X. (2017) FOXO1 inhibits the invasion and metastasis of hepatocellular carcinoma by reversing ZEB2-induced epithelial-mesenchymal transition. *Oncotarget* **8,** 1703–1713
42. Bowen, C., Ju, J.-H., Lee, J.-H., Paull, T. T., and Gelmann, E., P. (2013) Functional Activation of ATM by the prostate cancer suppressor NKX3.1. *Cell Reports* **4,** 516–529
43. Song, L.-N., Bowen, C., and Gelmann, E. P. (2013) Structural and functional interactions of the prostate cancer suppressor protein NKX3.1 with topoisomerase I. *Biochem. J.* **453,** 125–136
44. Bowen, C., Stuart, A., Ju, J. H., Tuan, J., Blonder, J., Conrads, T. P., Veenstra, T. D., and Gelmann, E. P. (2007) NKX3.1 homeodomain protein binds to topoisomerase I and enhances its activity. *Cancer Res.* **67,** 455–464
45. Mosquera, J. M., Mehra, R., Regan, M. M., Perner, S., Genega, E. M., Bueti, G., Shah, R. B., Gaston, S., Tomlins, S. A., Wei, J. T., Kearney, M. C., Johnson, L. A., Tang, J. M., Chinnaiyan, A. M., Rubin, M. A., and Sanda, M. G. (2009) Prevalence of TMPRSS2-ERG fusion prostate cancer among men undergoing prostate biopsy in the United States. *Clin. Cancer Res.* **15,** 4706–4711
46. Bowen, C., Zheng, T., and Gelmann, E. P. (2015) NKX3.1 suppresses TMPRSS2-ERG gene rearrangement and mediates repair of androgen receptor-induced DNA damage. *Cancer Res.* **75,** 2686–2698
47. Li, H., Ge, C., Zhao, F., Yan, M., Hu, C., Jia, D., Tian, H., Zhu, M., Chen, T., Jiang, G., Xie, H., Cui, Y., Gu, J., Tu, H., He, X., Yao, M., Liu, Y., and Li, J. (2011) Hypoxia-inducible factor 1 α-activated angiopoietin-like protein 4 contributes to tumor metastasis via vascular cell adhesion molecule-1/integrin β1 signaling in human hepatocellular carcinoma. *Hepatology* **54,** 910–919